Korean J. Chem. Eng., 40(12), 2876-2885 (2023)
DOI: 10.1007/s11814-023-1445-8

pISSN: 0256-1115
eISSN: 1975-7220

Catalytic hydrogenation of disinfection by-product bromate by cobalt and nickle prussian blue analogues with borohydride

Po-Hsin Mao*, Young-Kwon Park, Yi-Feng Lin***,†, Bui Xuan Thanh****, Duong Dinh Tuan*****, Afshin Ebrahimi******, Grzegorz Lisak*******,********, Thanit Tangcharoen*********, and Kun-Yi Andrew Lin*,†**

*Department of Environmental Engineering & Innovation and Development Center of Sustainable Agriculture, National Chung Hsing University, 250 Kuo-Kuang Road, Taichung, Taiwan
**School of Environmental Engineering, University of Seoul, Seoul 02504, Korea
***Department of Chemical Engineering and R&D Center for Membrane Technology, Chung Yuan Christian University, 200 Chung Pei Rd., Chungli, Taoyuan, Taiwan
****Faculty of Environment and Natural Resources, Ho Chi Minh City University of Technology, VNU-HCM, 268 Ly Thuong Kiet, District 10, Ho Chi Minh City, 700000, Viet Nam
*****International School, Thai Nguyen University, Thai Nguyen city, 250000, Viet Nam
******Environment Research Center and Department of Environmental Health Engineering Isfahan University of Medical Sciences Isfahan, Iran
*******Residues and Resource Reclamation Centre, Nanyang Environment and Water Research Institute, Nanyang Technological University, Singapore 637141, Singapore
********School of Civil and Environmental Engineering, Nanyang Technological University, Singapore 639798, Singapore
*********Department of Basic Science and Physical Education, Faculty of Science at Sriracha, Kasetsart University, Sriracha Campus, Chonburi, Thailand
(*Received 3 June 2022 • Revised 14 September 2022 • Accepted 31 January 2023*)

Abstract−As disinfection is employed extensively, disinfection by-product bromate has become an emerging environmental issue due to its carcinogenic toxicity. For developing an effective alternative approach for reducing bromate, cobalt and nickel-based Prussian Blue (PB) analogues are proposed here for incorporating a convenient reducing agent, $NaBH_4$ (i.e., a H_2-rich reagent) for reducing bromate to bromide as cobalt and nickel are recognized as effective metals for catalyzing hydrolysis of $NaBH_4$, and PB exhibits versatile catalytic activity. While CoPB and NiPB are comprised of the same crystalline structure, CoPB exhibits slightly higher specific surface area, more reductive surface, and more superior electron transfer than NiPB, enabling CoPB to accelerate bromate reduction. CoPB also exhibits a higher affinity towards $NaBH_4$ than NiPB based on density functional theory calculations. Moreover, CoPB also exhibits a relatively low activation energy (i.e., 59.5 kJ/mol) of bromate reduction than NiPB (i.e., 63.2 kJ/mol). Furthermore, bromate reduction by CoPB and NiPB could be also considerably enhanced under acidic conditions, and CoPB and NiPB could still effectively remove bromate even in the presence of nitrate, sulfate and phosphate. CoPB and NiPB are also validated to be recyclable for reducing bromate, indicating that CoPB and NiPB are promising heterogeneous catalysts for reducing bromate.

Keywords: Bromate, Catalytic Reduction, Bromide, Cobalt, Nickel, Prussian Blue

INTRODUCTION

As ozonation is increasingly employed for disinfection, numerous disinfection by-products have posed huge risks to public health and ecology due to their toxicity [1-3]. Among these disinfection by-products, bromate (BrO_3^-) has been one of the most important compounds, as BrO_3^- easily occurs from oxidation of bromide in water [4], which could be enhanced by photoactivation (i.e., sunlight exposure), and BrO_3^- is confirmed as a carcinogenic compound [5]. Recently, the occurrence of BrO_3^- has also been validated from various advanced oxidation processes, which are extensively employed for wastewater treatment [6,7]. Li et al. demonstrated that bromate can be formed in the presence of cobalt and peroxymonosulfate system, in which $SO_4^{\bullet-}$ is responsible for the oxidation of free bromide to bromate [7]. Liu et al. also found that bromide can be oxidized into bromate even in the absence of cobalt [6]. Therefore, developing effective methods for removing bromate is highly desired and urgent.

To date, several approaches have been already reported for removing bromate: adsorption, filtration, ion exchange, and membrane separation [8-20]. Among these approaches, filtration and membrane separation are much more favorable, as these approaches can

†To whom correspondence should be addressed.
E-mail: yflin@cycu.edu.tw, linky@nchu.edu.tw

be implemented continuously for treating a large quantity of wastewater. However, a concentrated bromate solution would be derived from these approaches which are designed to isolate and accumulate bromate, and thus, the toxicity of bromate still remains [21,22]. Thus, these concentrated bromate solutions would require further treatments to eliminate the toxicity before disposal. In addition to filtration and membrane separation, bromate may be also reduced via electrochemical method or photocatalytic method. Lu et al. investigated electrochemical reduction of bromate using carbon felt cathode modified by $Fe^{II}Al^{III}$ layered double hydroxide [23]. Tang and his co-workers developed a TiO_2/Ti_3C_2MXene composite for enhancing photocatalytic bromate reduction [24]. Nevertheless, these studies usually suffer from difficulties of complicated synthesis procedure and slightly low reduction efficiencies.

As bromate is a product of oxidation of bromide, reduction of bromate back to bromide through hydrogenation has become an attractive strategy for treating bromate [16,25-29]. Conventionally, hydrogenation of bromate is executed by purging H_2 gas into bromate solutions with usage of noble metal catalysts [30,31]. For example, Dong et al. employed activated carbon supported with ruthenium with continuous H_2 purge for reducing bromate [32]. Li and co-colleagues also prepared Pd supported on magnetite with different shells to catalyze hydrogenation of bromate [33]. However, since the solubility of H_2 gas in water is quite low, continuous H_2 purge would consume a large quantity of H_2 gas, and the safety issue of H_2 gas at large quantities would also pose a huge risk [30,31,34]. Thus, a much more controllable, more convenient, and safer hydrogenation process should be established. To this end, reducing agents, which would generate H_2 for hydrogenation reactions, would be promising alternative reductants. Borohydrides are promising candidates as they are considered as storage media of H_2 [35], and $NaBH_4$ can even have a relatively high H_2 capacity of ~11 wt%, which could be released through hydrolysis in mild conditions [36]. $NaBH_4$ is also a stable and non-flammable reagent, and thus $NaBH_4$ is considered as a safe and convenient source for releasing H_2 [37-39].

Nonetheless, H_2 generation from self-hydrolysis of $NaBH_4$ is extremely slow, and usually noble metal catalysts (e.g., Ruthenium, rhodium (Rd), and palladium (Pd)) are required to accelerate hydrolysis of borohydrides [40,41]. While Ru, Rd, and Pd are efficient catalysts for accelerating H_2 from borohydrides, these metals are noble metals at very high costs, impeding practical implementation of such a technique. Therefore, it would be much more advantageous to develop non-noble metal catalysts for catalyzing $NaBH_4$ for reducing bromate.

Among various non-noble metals, Co, and Ni are also validated as useful metals for catalyzing hydrolysis of $NaBH_4$ for generation of H_2 [42-44]. Therefore, development of Co, and Ni-based catalysts, which can catalyze hydrolysis of borohydride, and catalyze bromate reduction to bromide, would be attractive. To this end, metal-coordination materials with hierarchical structures, and porosity would be recognized as favorable candidates. As Prussian blue (PB) analogues represent the oldest coordination compounds [16], PB analogues, comprised of $M^{(II)}_2[M^{(III)}(CN)_6]$, contain the cyanide group, bridging two non-noble metal ions in octahedral sites to exhibit versatile and intriguing properties, making PB analogues highly versatile and advantageous in numerous catalytic reactions [34-36].

However, almost no existing studies are reported for investigating PBs, especially cobalt and nickel PBs for catalyzing hydrogenation of bromate using $NaBH_4$ as a reducing agent. Therefore, this present study attempts for the first time to examine and compare bromate hydrogenation using cobalt and nickel PBs for further elucidating their catalytic behavior and efficiency.

EXPERIMENTAL

All reagents in this study were used as received without additional purification, and the detailed information of reagents can be found in the supporting information. Preparation of PBs can be illustrated as shown in Fig. 1. Self-assembly of Co^{2+} or Ni^{2+} and $Fe(CN)_6^{3-}$ afforded PB ($Co_2[Fe(CN)_6]$, and $Ni_2[Fe(CN)_6]$).

Reduction of bromate using PB in the presence of borohydride was performed *via* batch-type experiments. In a typical experiment, 40 mg of $NaBH_4$ powder was dissolved in 0.2 L of DI water containing an initial concentration (C_0) (*e.g.*, 10 mg/L) of bromate. Subsequently, a certain amount of PB (*e.g.*, 50 mg) was added to the bromate solution under stirring at 30 °C. After pre-set intervals, sample aliquots were taken from the reactor and PB was promptly separated from the solution by filtration.

Concentrations of bromate and resulting bromide were then mea-

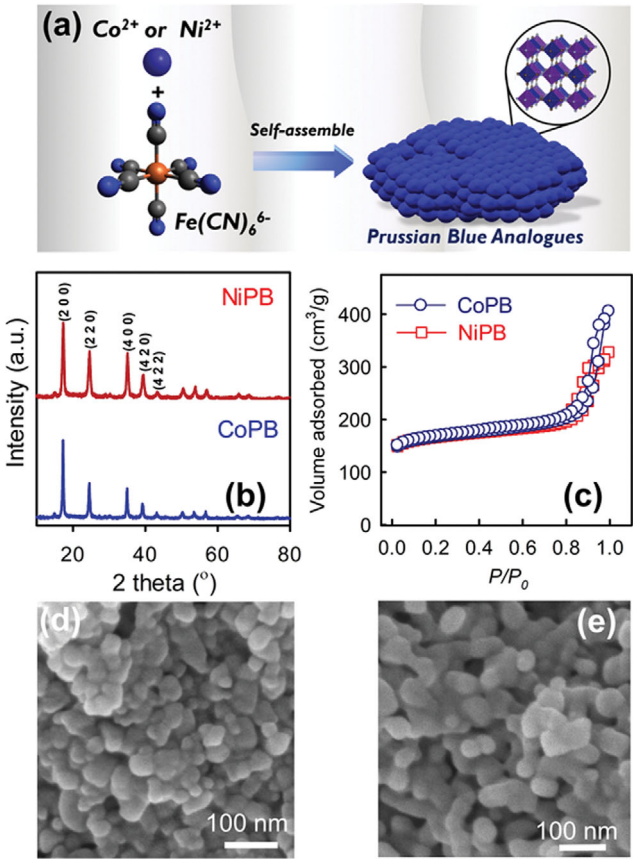

Fig. 1. (a) Preparation of CoPB and NiPB, (b) XRD, and (c) N_2 sorption isotherms of PBs; SEM images of (d) CoPB, and (e) NiPB.

sured by an ion chromatography system (Dionex IC System, USA). Conditions included a column: Dionex IonPac AS9-HC Analytic (4×250 nm), eluent: 9 mM Na_2Co_3, suppressor: Dionex anion self-regenerating suppressor, current: 45 mA, injection volume: 25 μL. The effect of catalyst dosage on hydrogenation of bromate was investigated by changing the amount of PB added from 150 mg/L to 350 mg/L. These concentrations were particularly selected based on reported studies in literature [45,46]. The effect of initial temperatures of bromate solution was also verified by altering solution's temperature from 30 °C to 50 °C, in which the temperature of the reactor was controlled by a hot stirring plate. The effect of co-existing anions (e.g., nitrate, sulfate, phosphate) was examined by adding the equivalent concentration (i.e., 10 mg/L) to bromate solution. Recyclability of PB for bromate reduction was performed by reusing recovered PB without any regeneration treatments. Bromate removal efficiency and bromide production efficiency are calculated by the following equation:

$$q_t = \frac{v|C_0 - C_t|}{M} \quad (1)$$

where M (g) is the amount of PB used in the reduction experiment and v (L) is the total volume of solution. C_0 and C_t are the concentration of bromate (or bromide) in the beginning and at a certain reaction time t in mmol/L. The q_e was adopted to denote bromate removal efficiency and bromide production efficiency at equilibrium. An initial concentration of bromate at 10 mg/L (i.e., 0.078 mM) was adopted because this concentration has been frequently tested in literature [46-48].

RESULTS AND DISCUSSION

1. Characterization of PB

To first validate the successful preparation of CoPB and NiPB, their XRD patterns were measured, and displayed in Fig. 1(a). Both CoPB and NiPB exhibited the typical pattern of conventional PB with signature peaks at 17, 24, 35, 39 and 43°, corresponding to (2 0 0), (2 2 0), (4 0 0), (4 2 0) and (4 2 2) planes of PB [39]. Such a pattern was ascribed to the cubic $M^{II}_2[Fe(CN)_6]$ framework, consisting of an octahedral $[Fe(CN)_6]$ complex coordinated with nitrogen-bound Fe^{III} ions. Therefore, PBs were iso-structurally crystallized in the space group of *Fm3m* [27,40].

In addition to the crystalline structure of as-prepared PBs, the morphologies of CoPB and NiPB were then characterized in Fig. 1(d)-(e), in which CoPB and NiPB revealed a very comparable morphology, consisting of rounded particles with sizes of a few tens of nanometers. Very small voids were also found between the rounded particles. Textural properties of these PBs were also analyzed as shown in Fig. 1(c). These two PBs actually showed comparable sorption isotherms as the IUPAC type IV with a small hysteresis loop, indicating the existence of pores as observed in the SEM images. Both CoPB and NiPB could enable large amounts of N_2, but CoPB seemed to adsorb a relatively large amount of N_2. Therefore, CoPB exhibited a slightly higher surface area of 522 m^2/g, whereas NiPB showed a slightly lower surface of 502 m^2/g. Through the characterizations of morphological and textural analyses, CoPB was slightly different from NiPB.

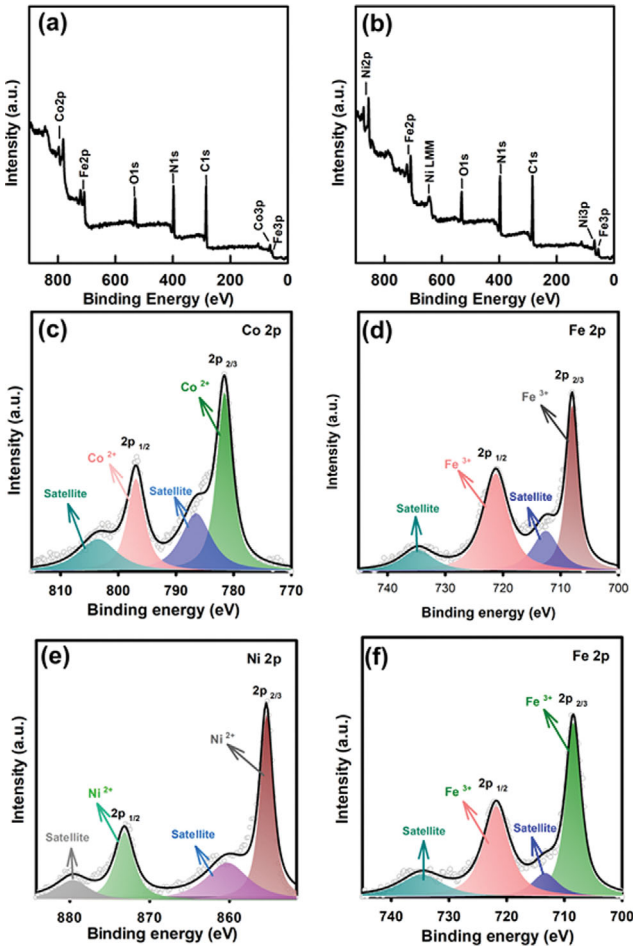

Fig. 2. XPS analyses of PBs: Full survey scans of (a) CoPB, and (b) NiPB; core level spectra of (c) Co2p and (d) Fe2p of CoPB, and core level spectra of (e) Ni2p, and (f) Fe2p.

Additionally, surface chemistry of these PBs was then determined using XPS. Fig. 2(a) displays the full survey spectrum of CoPB, in which significant fractions of Co, and Fe could be detected, whereas Fig. 2(b) reveals the full survey spectrum of NiPB comprised of noticeable amounts of Ni, and Fe. In particular, the Co2p core-level spectrum of CoPB (Fig. 2(c)) can be then deconvoluted to afford two peaks at 781.4, and 796.8 eV, attributed to Co^{2+}, which is the theoretical species of Co in $Co_2[Fe(CN)_6]$ [49]. On the other hand, Fig. 2(d) shows the core-level Fe2p spectrum, in which two peaks would be also unveiled after deconvolution at 707.8, and 721.0 eV, corresponding to Fe^{3+} species. In the case of NiPB, Fig. 2(e) reveals the Ni2p core-level spectrum, in which two peaks at 855.4, and 873.2 eV, ascribed to Ni^{2+} species formulated in $Ni_2[Fe(CN)_6]$. On the other hand, Fig. 2(f) shows the Fe2p core-level spectrum, which would be then deconvoluted to display two peaks at 708.3, and 721.8 eV, corresponding to Fe^{3+} [49]. These XPS results validate the formation of PBs, in which multi-valence metal species would co-exist.

2. Catalytic Bromate Reduction Using PB in the Presence of $NaBH_4$

As bromate is possibly removed via adsorption, it is essential to

verify whether bromate can be removed due to adsorption to PB. Fig. 3(a) firstly reveals that when CoPB alone was present, the concentration of bromate was barely changed after 120 min, demonstrating that bromate would not be removed by CoPB via adsorption. Moreover, it would be also necessary to examine whether the reducing agent, $NaBH_4$, itself would remove bromate. Nonetheless, the concentration of bromate in the presence of $NaBH_4$ only was negligibly decreased over 120 min, suggesting that the reducing agent without catalysts could not effectively eliminate bromate, possibly because H_2 released from self-hydrolysis of $NaBH_4$ without catalysts was very ineffective [43,50].

Subsequently, when CoPB at 150 mg/L was combined with $NaBH_4$, the concentration of bromate rapidly decreased, and C_t/C_0 approached 0.2 in 120 min, suggesting that bromate might be eliminated by CoPB+$NaBH_4$. Moreover, once the dosage of CoPB was further increased to 250 mg/L, the concentration of bromate decreased even more rapidly, and then was completely eliminated in 120 min. At the dosage of CoPB=300 mg/L, the elimination of bromate proceeded even much faster. As CoPB, and $NaBH_4$ could not effectively remove bromate individually, these results demonstrated that CoPB combined with the reducing agent, $NaBH_4$, would remove bromate, and a higher dosage of CoPB would lead to more efficient and faster bromate removal.

For further investigating the effect of CoPB dosage, the corresponding bromate removal efficiency was than calculated in terms of μmol/g-CoPB as shown in Fig. 3(b). At CoPB=150 mg/L, the removal efficiency increased gradually from zero to 430 μmol/g at 120 min. More importantly, Fig. 3(c) shows that bromide could be also correspondingly generated during bromate reduction. This verified that the combination of CoPB successfully reduced bromate and converted it to bromide. Nevertheless, one can note that the kinetics of bromide production seemed slightly different (slower) from that of bromate reduction, and the amount of bromide produced was also slightly lower than that of bromate reduced. This phenomenon has been also observed in previous studies, as bromate reduction and transformation to bromide using heterogeneous catalysts inevitably involves interfacial interactions and transformation of reactants [20,28-30,50,52]. Therefore, the as-produced bromide (or intermediates) might reside on surface of catalysts, leading to the delayed kinetics [20,29,53,54].

When CoPB dosage increased to 250 mg/L, its bromate removal efficiency became slightly lower because bromate present in the solution had been completely eliminated, and the calculation of bromate removal efficiency adopted a much higher value of CoPB dosage as the denominator. Similar results can be also observed in the case of CoPB=350 mg/L, and even lower efficiency would be afforded owing to a relatively high dosage of CoPB present. Nevertheless, since CoPB at 150 mg/L could not fully eliminate and reduce bromate (0.078 μM) present in the solution, and CoPB at 250 mg/L and 350 mg/L would lead to similar bromate removal efficiency, the dosage of 250 mg/L appeared as an appropriate dosage of CoPB for bromate reduction.

On the other hand, when NiPB was employed, NiPB only (without $NaBH_4$) could not noticeably remove bromate through adsorption either as shown in Fig. 4(a). As $NaBH_4$ and NiPB individually could not effectively remove bromate, bromate concentration can be

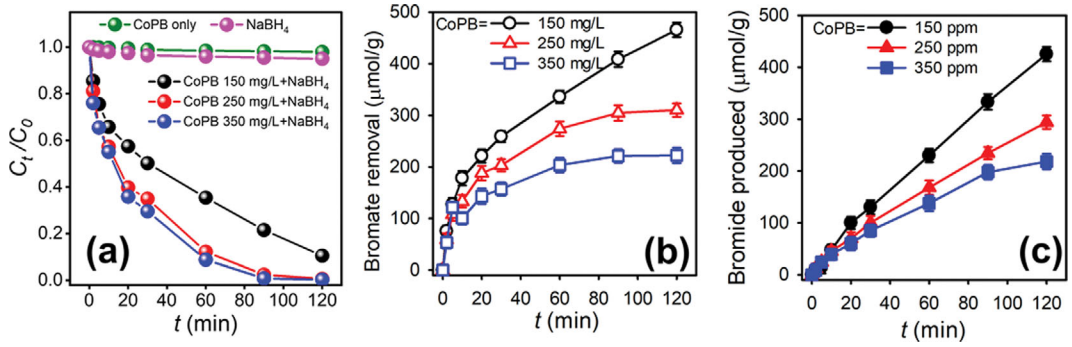

Fig. 3. Effect of CoPB dosage on (a) variation of bromate, (b) bromate removal efficiency, and (c) bromide production efficiency (T=30 °C).

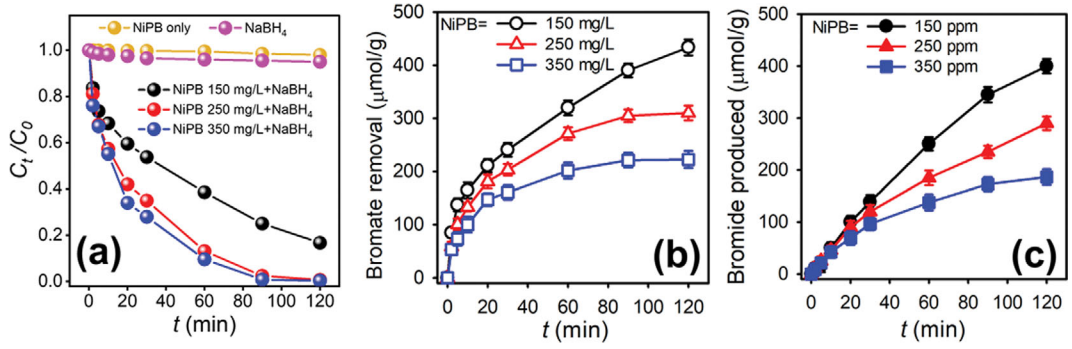

Fig. 4. Effect of NiPB dosage on (a) variation of bromate, (b) bromate removal efficiency, and (c) bromide production efficiency (T=30 °C).

rapidly decreased in the presence of NiPB at 150 mg/L and $NaBH_4$.

Once the dosage of NiPB increased to 250 mg/L, bromate concentration decreased even more rapidly and was completely removed in 120 min. Similar results can be also obtained with faster complete removal of bromate by 350 mg/L of NiPB. Fig. 4(b) further displays bromate removal efficiency (μmol/g-NiPB) at different dosages. The dosage of 150 mg/L could also enable a high removal efficiency, and the correspondingly produced bromide could be observed as shown in Fig. 4(c), indicating that NiPB with $NaBH_4$ can also successfully reduce bromate and convert it to bromide. Nevertheless, the delayed kinetics and a slightly lower amount of bromide was observed at the end of the reaction, suggesting that the as-produced bromide (or intermediates) might reside on surface of catalysts, leading to the delayed kinetics [20,28,53,54].

On the other hand, NiPB at 150 mg/L could not fully eliminate and reduce bromate (0.078 μM) present in the solution either, and NiPB at 250 mg/L and 350 mg/L would lead to similar bromate removal efficiencies. Therefore, the dosage of 250 mg/L would be considered as an appropriate dosage of NiPB for bromate reduction. Thus, the dosage of 250 mg/L would be then selected for investigating other effects over the course of this study.

While both CoPB and NiPB at 250 mg/L successfully enabled the full removal of bromate and reduced bromate to bromide, it would be interesting to further compare these two PBs. Especially, for distinguishing their kinetics for bromate removal in terms of removal efficiency (q_t), the pseudo-first-order rate law was then adopted as follows:

$$q_t = q_e(1 - e^{-k_{obs}t}) \quad (2)$$

where q_t is bromate removal efficiency at time t, q_e is the removal efficiency for bromate at equilibrium, and k_{obs} is the "observed" pseudo-first-order rate constant (min^{-1}). As k_{obs} for bromate removal by CoPB was then calculated as 0.053 min^{-1}, the corresponding k_{obs} for bromate removal by NiPB was determined as 0.050 min^{-1}, suggesting that CoPB seemed to enable a slightly faster bromate reduction than NiPB.

The effect of different $NaBH_4$ concentrations was investigated in Fig. S1 by changing $NaBH_4$ concentration from 100 to 300 mg/L. When $NaBH_4$ concentration increased from 200 to 300 mg/L, bromate reduction using both CoPB, and NiPB was slightly accelerated, as their rate constants became higher to 0.077, and 0.064 min^{-1}, respectively. On the other hand, once $NaBH_4$ concentration was lowered to 100 mg/L, bromate reduction became less efficient using both CoPB, and NiPB, possibly due to the low availability of hydrogen gas from $NaBH_4$. These results further demonstrated that the availability of hydrogen from $NaBH_4$ would influence bromate reduction, and a higher $NaBH_4$ concentration would enhance bromate reduction kinetically.

Conventionally, the reducing agent, $NaBH_4$, would be hydrolyzed for generating hydrogen molecule as follows [55,56]:

$$NaBH_4 + 2H_2O \rightarrow NaBO_2 + 2H_2 \quad (3)$$

H_2 has been validated to play an important role for reducing bromate to bromide through the following reaction (Eq. (3)):

$$BrO_3^- + 3H_2 \xrightarrow{Catalysts} Br^- + 3H_2O \quad (4)$$

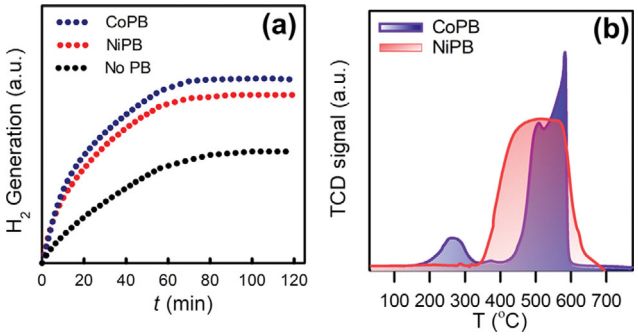

Fig. 5. (a) H_2-TPR profiles, and (b) H_2 generation of $NaBH_4$ ($NaBH_4$ (6.6 mM) by CoPB, and NiPB.

Therefore, H_2 evolution from $NaBH_4$ catalyzed by CoPB, and NiPB might offer insights into understanding bromate reduction by PB together with $NaBH_4$. Fig. 5(a) shows that the self-hydrolysis of $NaBH_4$ for releasing H_2 was extremely slow. Nevertheless, H_2 evolution by $NaBH_4$ in the presence of PBs became significantly faster in the beginning and gradually reached equilibrium. Interestingly, the trend of H_2 evolution was similar to the trend of bromate removal. These results suggested that removal of bromate by PB+$NaBH_4$ would be related to the reaction expressed in Eq. (3), which could occur through a few possible processes [25].

In the first process, bromate might still temporarily reside on the surface of PB and react with H_2 molecules from $NaBH_4$ to transfer into bromide as the first route in Fig. 6. Moreover, as PB contained M^{2+}, these M^{2+} species would donate electrons to bromate and convert it to bromide, while these M^{2+} species would be reduced back to their original reductive states by H_2 [25] as the second route in Fig. 6.

While both CoPB and NiPB can successfully catalyze hydrolysis of $NaBH_4$ for H_2 evolution, CoPB seemed to enable a noticeably faster H_2 evolution, especially in the beginning. This feature might be correlated to the faster k_{obs} of bromate removal obtained by CoPB than NiPB, possibly because CoPB could enable a much faster H_2 evolution from accelerating hydrolysis of $NaBH_4$. A number of studies have also revealed that Co would exhibit a higher catalytic activity than Ni for hydrolyzing $NaBH_4$ for H_2 production [58,59]. This comparison further validated that bromate reduction by PB was certainly involved with H_2 generation by $NaBH_4$, and H_2 would then react with bromate and reduce cobalt species to convert bromate to bromide.

To further probe into this difference, theoretical calculations based on the density functional theory (DFT) were conducted to examine interactions (especially, adsorption processes) between $NaBH_4$, and PBs. Since CoPB and NiPB exhibited a main plane of (200), the (200) plane of each PB was adopted as a representative surface plane of PB based on their XRD patterns. Fig. 7(a) shows a side-view of CoPB(200), on which a molecule of BH_4^- ion approaching the (200) surface of CoPB, and the adsorption energy of BH_4^- to CoPB(200) could be calculated as follows:

$$\text{Adsorption energy} = E_{BH_4^-@CoPB(200)} - E_{CoPB(200)} - E_{BH_4^-} \quad (5)$$

Then, the adsorption energy of BH_4^- to CoPB(200) was calculated as −3.11 eV, and such a negative value indicated that BH_4^- ion

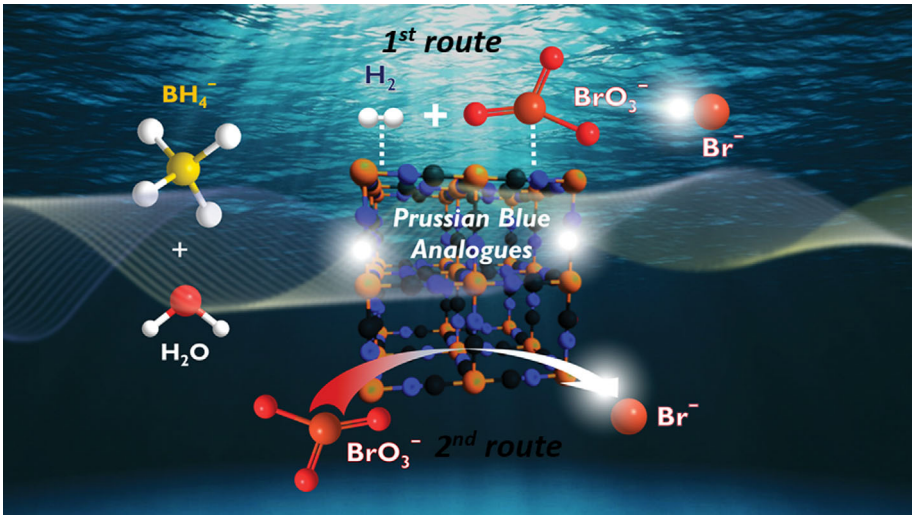

Fig. 6. Proposed mechanisms for bromate reduction to bromide by PB in the presence of $NaBH_4$.

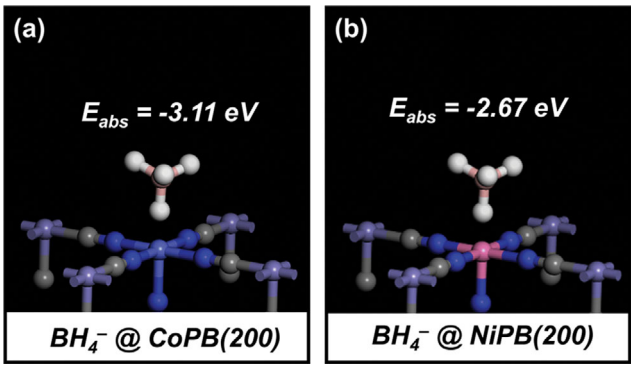

Fig. 7. DFT calculation: (a) side-view of adsorption of BH_4^- to CoPB alone the (200) plane, and (b) side-view of adsorption of BH_4^- to NiPB alone the (200) plane.

showed a high affinity towards CoPB surface along the (200) plane. In the case of NiPB, Fig. 7(b) also depicts the molecule of BH_4^- approaching the dominant (200) plane of NiPB, and the resulting adsorption energy of BH_4^- to CoPB(200) would be calculated via Adsorption energy$=E_{BH_4^-@NiPB(200)}-E_{NiPB(200)}-E_{BH_4^-}$ as −2.67 eV. This also confirmed that BH_4^- ion showed a high affinity towards NiPB surface along the (200) plane. However, the much more negative adsorption energy of BH_4^- to CoPB than that to NiPB might demonstrate that the adsorption process of BH_4^- to CoPB could be even more favorable than that to NiPB. This might a possible reason for elucidating why bromate reduction by CoPB+$NaBH_4$ was faster than that by NiPB+$NaBH_4$.

On the other hand, redox properties of these PB also seemed to play an important role in reducing bromate, especially through mediated reduction with H_2. Therefore, H_2-temperature-programmed reduction (H_2-TPR) profiles of these PBs were measured in Fig. 5(b). Even though CoPB and NiPB both consisted of the same formula as $M^{II}[Fe(CN)_6]$, their H_2-TPR profiles were noticeably different. In particular, a noticeable reduction peak of CoPB happened at a relatively low temperature of 270 °C and NiPB would not show any reduction peaks below 300 °C. Such comparisons

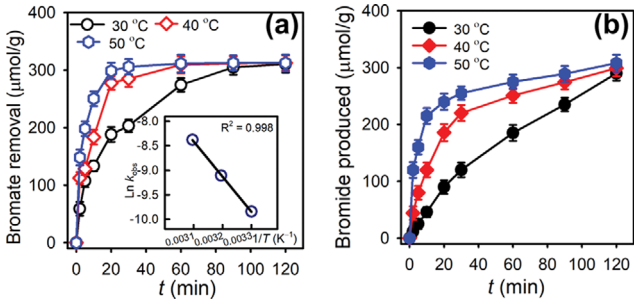

Fig. 8. Effect of temperature on (a) bromate removal efficiency, and (b) bromide production efficiency by using CoPB.

indicate that the surface of CoPB might possess sites which would be more easily reduced than NiPB, thereby enhancing its activity for reducing bromate.

Cyclic voltammetry (CV) curves of CoPB and NiPB were also obtained to distinguish electrochemical properties of CoPB and NiPB in Fig. S2. CoPB seems to exhibit a slightly higher current density and reductive capability than NiPB, suggesting that CoPB might possess more advantageous activity for reducing bromate.

3. Effect of Temperature on Bromate Reduction

Furthermore, since temperature is an essential parameter for $NaBH_4$ hydrolysis [50,59,60] and kinetics of bromate reduction might be influenced at different temperatures, the effect of temperature was subsequently examined. Fig. 8(a) displays the effect of temperature on bromate reduction using CoPB at 30, 40, and 50 °C. When a higher temperature was adopted, bromate removal advanced much more rapidly to reach equilibrium, suggesting that a relatively high temperature seemed to accelerate bromate reduction. The k_{obs} of bromate removal by CoPB at 30 °C was 0.053 min^{-1}, which would increase to 0.110, and 0.230 min^{-1} as temperature rose up from 30 to 40 and 50 °C, respectively. Similarly, the same phenomenon was also observed in the case of bromide production efficiency (q_t) at increasing temperatures (Fig. 8(b)).

Moreover, as the k_{obs} of bromate removal increased at rising temperature, the relationship of k_{obs} of bromate reduction and tem-

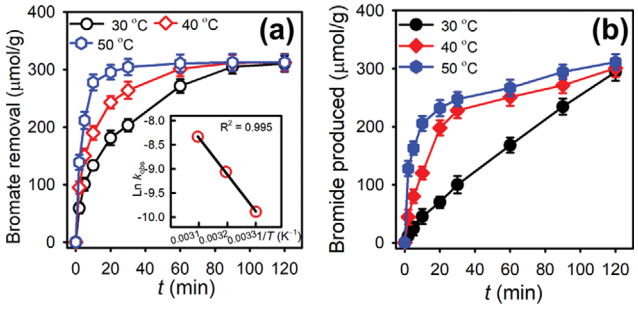

Fig. 9. Effect of temperature on (a) bromate removal efficiency, and (b) bromide production efficiency by using NiPB.

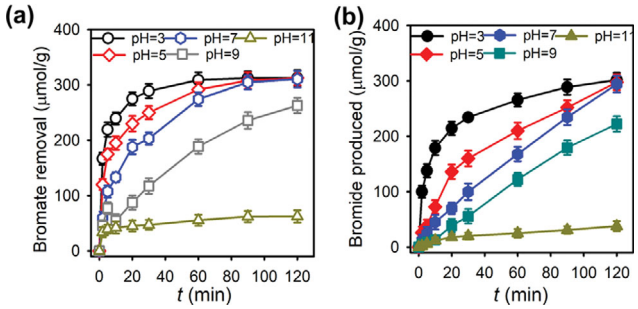

Fig. 10. Effect of pH on (a) bromate removal efficiency, and (b) bromide production efficiency by using CoPB (30 °C).

perature would then correspond via the Arrhenius equation as follows (Eq. (6)):

$$\ln k_{obs} = \ln A - E_a/RT \quad (6)$$

where E_a is the activation energy (kJ/mol) for the bromate reduction, A is the temperature-independent factor (g/mg/min); R represents the universal gas constant and T is the solution temperature in Kelvin (K). A plot of ln k_{obs} versus 1/T was depicted as the inset in Fig. 8(a). The data points could be well fit by the linear regression (R^2=0.998), indicating that the kinetics of bromate removal can correspond to temperature through the Arrhenius equation. The corresponding E_a was then calculated as 59.5 kJ/mol.

On the other hand, Fig. 9(a) shows the effect of temperature on bromate removal using NiPB at different temperatures, and bromate removal also proceeded much more rapidly to reach equilibrium at a higher temperature. The corresponding k_{obs} at 30 °C was 0.050 min^{-1}, which would increase to 0.116 min^{-1}, and 0.240 min^{-1} at 40, and 50 °C, respectively. The resulting bromide production also advanced much more quickly at higher temperatures, affirming the enhancing effect of higher temperature on bromate reduction.

The inset in Fig. 9(a) also reveals a plot of lnk_{obs} of bromate removal versus 1/T, and the data points were also well-fitted by the linear regression with a R^2=0.995. The corresponding E_a was then determined as 63.2 kJ/mol. In comparison with the E_a by NiPB, the E_a by CoPB seemed slightly lower, suggesting that the catalytic activity of CoPB might be higher than NiPB for bromate removal, possibly because of the more active surface for reductive reactions as discussed earlier.

Comparatively, a previous study by Nurlan et al. [45] using Ni(bipy)(1,3,5-BTC) and $NaBH_4$ for bromate reduction, and reported a rate constant of 0.053 min^{-1}, which, however, was achieved using a significantly higher dosage of $NaBH_4$ (i.e., 500 mg/L) at the same dosage of catalyst. This comparison further indicates that CoPB and NiPB appeared to be more efficient catalysts than other reported catalysts for bromate reduction.

4. Effects of pH and Co-existing Anions on Bromate Reduction

As bromate reduction is an aqueous reaction, pH has been also an important factor. Therefore, the effect of pH on bromate removal was examined by varying pH of bromate solutions to 3-11. Fig. 10(a) displays bromate removal at different pH values, showing that bromate reduction was significantly influenced by various pH. In particular, when the bromate solution was varied from the neutral condition to a relatively acidic condition at pH=5, bromate removal was noticeably improved as its kinetics changed slightly faster and k_{obs} increased from 0.053 to 0.070 min^{-1}. Likewise, the resulting bromide production also proceeded noticeably faster (Fig. 10(b)).

Once the pH was lowered to 3, the more acidic condition, the k_{obs} became even faster to 0.316 min^{-1}, indicating the acidic conditions would facilitate bromate reduction. However, when pH changed from the neutral condition to the relatively alkaline condition at pH=9, bromate removal was noticeably hindered, and the overall bromate removal efficiency at 120 min was decreased to from 310 to 262 μmol/g; the corresponding k_{obs} also decreased to 0.019 min^{-1}. Simultaneously, the resulting bromide production was also slightly decreased. Once pH further increased to 11, the adverse effect seemed to become even more pronounced as the bromate removal efficiency dropped considerably to 62.5 μmol/g, and the resulting bromide production was noticeably suppressed. These results indicate that alkaline conditions would negatively influence bromate removal by CoPB.

Similar results can be also observed in the case of NiPB in Fig. 11(a), in which bromate removal would proceed much faster to reach equilibrium at pH=5, and pH=3, as their k_{obs} increased from 0.051 to 0.062, and 0.265 min^{-1}, respectively.

Once pH changed from the neutral condition to the alkaline condition at pH=9, bromate removal was notably suppressed, and the overall bromate removal efficiency at 120 min dropped from 310 to 259 μmol/g; the corresponding k_{obs} was also reduced to 0.022 min^{-1} with a notable decrease in the resulting bromide pro-

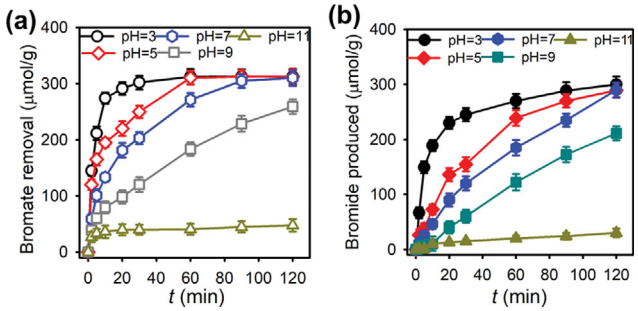

Fig. 11. Effect of pH on (a) bromate removal efficiency, and (b) bromide production efficiency by using NiPB (30 °C).

duction. Next, when pH increased to 11, such negative effects were even more intense as the bromate removal efficiency decreased significantly to 47.3 μmol/g, and the resulting bromide production was inhibited.

These results indicate that the effect of pH had a considerable impact on bromate removal using PBs, possibly attributed to several reasons. First, since bromate reduction would occur via reactions between bromate ions on the surface of PB and H_2 as depicted in Fig. 6 as the second route. As PB exhibited a relatively positive surface charge under acidic conditions (Fig. S3), the attraction between BrO_3^- and PB was intensified, thereby favoring contact between bromate and PB. In contrast, the alkaline condition might cause PB surface to exhibit more negative charge, and thus the resultant more intense repulsion between BrO_3^- and PB, hindering contact between bromate, and PB [16,28]. On the other hand, the alkaline condition would also cause competition between hydroxyl anions, BrO_3^- as well as BH_4^- from $NaBH_4$ for further reactions, thereby decreasing bromate reduction efficiency [61,62]. Additionally, H_2 evolution from $NaBH_4$ hydrolysis might be also under alkaline conditions [43,63]. Therefore, overall bromate removal efficiency was less effective in alkaline environment.

Besides, since bromate-containing wastewaters might also contain other ions, especially anions, including nitrate, phosphate and sulfate, it would be essential to examine how these conventional anions affected bromate removal by PB. Prior to investigating the effect of different anions, a mixture of bromate with nitrate, phosphate and sulfate at the same concentration (i.e., 10 mg/L) was prepared. Fig. 12(a) reveals bromate removal efficiency and the resulting bromide production efficiency using CoPB in the presence of other anions. Overall, bromate could be still removed and converted to bromide; nevertheless, the bromate removal efficiency at 120 min was 291 μmol/g, which was slightly lower than that in the absence of anions as 310 μmol/g. The presence of these anions might lead to the competing effect as nitrate, phosphate and sulfate could be also removed by CoPB, possibly due to adsorption. Nevertheless, even though there were several anions present in the system, CoPB was still capable of removing a significant fraction of bromate and converting it to bromide.

On the other hand, Fig. 12(b) also reveals bromate removal in the presence of these anions using NiPB. These co-existing anions would be also removed by NiPB, especially nitrate, thereby causing the possible competing effect to bromate removal as the corresponding bromate removal efficiency was slightly reduced to 287 μmol/g. Nevertheless, a large portion of bromate was still successfully removed by NiPB, and converted to bromide using NiPB. These results by CoPB, and NiPB both demonstrated that CoPB and NiPB could still reduce bromate even in the presence of co-existing anions.

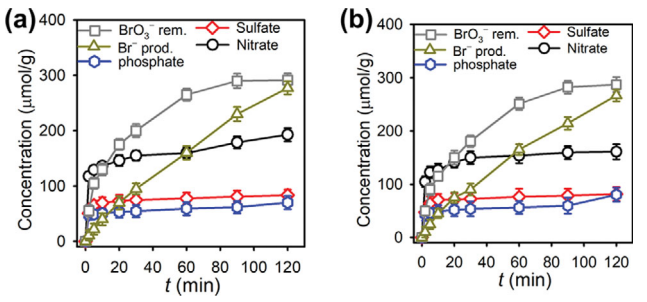

Fig. 12. Effect of anions on bromate removal efficiency, and bromide production efficiency by using (a) CoPB and (b) NiPB (30 °C).

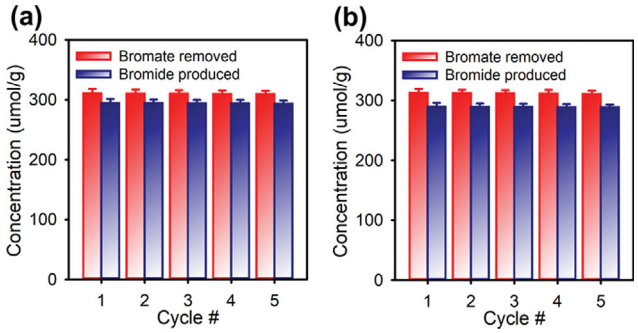

Fig. 13. Recyclability of (a) CoPB, and (b) NiPB for bromate removal (30 °C).

5. Recyclability of PB for Bromate Reduction

Since PBs would be employed as heterogeneous catalysts for bromate reduction, it was critical to evaluate its reusability. Fig. 13(a) shows bromate removal efficiency, and bromide production efficiency of consecutive five cycles at equilibrium using CoPB. Overall, bromate could be constantly and efficiently removed and converted to bromide without substantial changes. Similar results can be also observed in the case of NiPB (Fig. 11(b)), showing that NiPB would also enable the continuous five cycles of bromate removal, and conversion to bromide without noticeable losses. These results demonstrate that PBs would be reusable, and exhibit stable activity for reducing bromate to bromide over multiple cycles.

To further examine stability of these PBs, the cyanide concentration after the recyclability test was also analyzed using the spectrophotometric method with a pyridine-barbituric acid reagent [64,65] for determining whether cyanide ion might be present and derived from CoPB, and NiPB. Nevertheless, the concentration of cyanide detected in the solution by the spectrophotometric method was below the detection limit, in both cases of CoPB, and NiPB, suggesting that cyanide was not released from PB.

We are also aware of the possibility of releasing cyanide, Co, and Ni ions.

Moreover, the concentrations of cobalt, and nickel in the solution after the recyclability test were measured using ICP-MS. The concentrations of cobalt and nickel were determined as 0.003 mg/L and 0.005 mg/L, respectively. These concentrations were much lower than the amount of CoPB and NiPB used in this study (i.e., 250 mg/L), indicating that releasing of Co or Ni from PB was negligible. Fig. S4 also reveals the XRD patterns of spent PBs, which were very comparable to those of original PBs, indicating that these PBs were durable and recyclable for catalytic bromate reduction.

CONCLUSION

For developing an effective alternative approach for reducing the toxic disinfection by- product, bromate, cobalt and nickel-based

PBs are proposed for incorporating $NaBH_4$ for reducing bromate to bromide. While CoPB and NiPB are comprised of the same crystalline structure and capable of reducing bromate to bromide, CoPB exhibited slightly a specific surface area, more reductive surface, and more superior electron transfer than NiPB, enabling CoPB to accelerate bromate reduction. Moreover, CoPB also exhibited a relatively low activation energy of bromate reduction than NiPB. Furthermore, bromate reduction by CoPB and NiPB could be also considerably enhanced under the acidic conditions, and CoPB and NiPB could still effectively remove bromate even in the presence of nitrate, sulfate and phosphate. CoPB and NiPB were also validated to be recyclable for reducing bromate, indicating that CoPB and NiPB are promising heterogeneous catalysts for reducing bromate.

ACKNOWLEDGEMENTS

The authors are grateful for the funding granted from the Ministry of Science and Technology, and technical support from the National Center for High-Performance Computing, Taiwan. The authors gratefully acknowledge the use of SQUID000200 of MOST111-2731-M-006-001 belonging to the Core Facility Center of National Cheng Kung University.

SUPPORTING INFORMATION

Additional information as noted in the text. This information is available via the Internet at http://www.springer.com/chemistry/journal/11814.

REFERENCES

1. A. Chin and P. R. Bérubé, *Water Res.*, **39**, 2136 (2005).
2. P. Deeudomwongsa, S. Phattarapattamawong and K. Y. A. Lin, *Chemosphere*, **184**, 1215 (2017).
3. I. A. Ike, Y. Lee and J. Hur, *Chem. Eng. J.*, **375**, 121929 (2019).
4. M. R. Khan, Z. A. Alothman, N. J. Alqahtani, I. H. Alsohaimi and M. Naushad, *Anal. Methods*, **6**, 4038 (2014)
5. U. Pinkernell and U. von Gunten, *Environ. Sci. Technol.*, **35**, 2525 (2001).
6. K. Liu, J. Lu and Y. Ji, *Water Res.*, **84**, 1 (2015).
7. Z. Li, Z. Chen, Y. Xiang, L. Ling, J. Fang, C. Shang and D. D. Dionysiou, *Water Res.*, **83**, 132 (2015).
8. J. A. Wiśniewski and M. Kabsch-Korbutowicz, *Desalination*, **261**, 197 (2010).
9. A. Bhatnagar, Y. Choi, Y. Yoon, Y. Shin, B.-H. Jeon and J.-W. Kang, *J. Hazard. Mater.*, **170**, 134 (2009).
10. K. Listiarini, J. T. Tor, D. D. Sun and J. O. Leckie, *J. Membr. Sci.*, **365**, 154 (2010).
11. M. Naushad, Z. A. ALOthman, M. R. Khan and S. M. Wabaidur, *Clean*, **41**, 528 (2013).
12. M. Naushad, M. R. Khan, Z. A. Alothman and M. R. Awual, *Desalination Water Treat.*, **57**, 5781 (2016).
13. M. Naushad, P. Senthil Kumar and S. Suganya, *Bromate formation in drinking water and its control using graphene based materials*, in: M. Naushad (Ed.) A New Generation Material Graphene: Applications in Water Technology, Springer International Publishing, Cham, 239 (2019).
14. A. Sharma, G. Sharma, M. Naushad and D. Pathania, *J. Chil. Chem. Soc.*, **61**, 2940 (2016).
15. M. Naushad, M. R. Khan, Z. A. Alothman, I. AlSohaimi, F. Rodriguez-Reinoso, T. M. Turki and R. Ali, *Environ. Sci. Pollut. Res. Int.*, **22**, 15853 (2015).
16. K.-Y. A. Lin and C.-H. Lin, *Chem. Eng. J.*, **297**, 19 (2016).
17. K.-Y. A. Lin and C.-H. Lin, *Chem. Eng. J.*, **325**, 144 (2017).
18. K.-Y. A. Lin, C.-H. Lin and J.-Y. Lin, *J. Colloid Interface Sci.*, **504**, 397 (2017).
19. K.-Y. A. Lin, J.-Y. Lin and H.-L. Lien, *Chemosphere*, **172**, 325 (2017).
20. Y.-T. Chiu, P.-Y. Lee, T. Wi-Afedzi, J. Lee and K.-Y. A. Lin, *J. Colloid Interface Sci.*, **532**, 416 (2018).
21. S. Kliber and J. A. Wiśniewski, *Desalination Water Treat.*, **35**, 158 (2011).
22. M. Moslemi, S. H. Davies and S. J. Masten, *Environ. Eng. Sci.*, **29**, 1092 (2012).
23. Z. Lu, Q. Yang, T. Hu, J. Wang and W. Tang, *Chem. Eng. J.*, **446**, 137356 (2022).
24. S. Tang, J. Yao, H. Liu and Y. Zhang, *J. Environ. Chem. Eng.*, **10**, 107099 (2022).
25. J. Restivo, O. S. G. P. Soares, J. J. M. Órfão and M. F. R. Pereira, *Chem. Eng. J.*, **263**, 119 (2015).
26. P. Zhang, F. Jiang and H. Chen, *Chem. Eng. J.*, **234**, 195 (2013).
27. K.-Y. A. Lin, C.-H. Lin, S.-Y. Chen and H. Yang, *Chem. Eng. J.*, **303**, 596 (2016).
28. K.-Y. A. Lin, C.-H. Lin and H. Yang, *J. Environ. Chem. Eng.*, **5**, 5085 (2017).
29. B.-C. Li, H. Yang, E. Kwon, D. Dinh Tuan, T. Cong Khiem, G. Lisak, B. Xuan Thanh, F. Ghanbari and K.-Y. Andrew Lin, *Sep. Purif. Technol.*, 119320 (2021).
30. N. Nurlan, A. Akmanova and W. Lee, *Nanomaterials*, **12**, 1212 (2022).
31. Z. Dong, F. Sun, W. Dong and C. Jiang, *Environ. Eng. Sci.*, **35**, 176 (2018).
32. Z. Dong, W. Dong, F. Sun, R. Zhu and F. Ouyang, *React. Kinet., Mech. Catal.*, **107**, 231 (2012).
33. M. Li, X. Zhou, J. Sun, H. Fu, X. Qu, Z. Xu and S. Zheng, *Sci. Total Environ.*, **663**, 673 (2019).
34. Y.-T. Chiu, H. Wang, J. Lee and K.-Y. A. Lin, *Process Saf. Environ. Prot.*, **127**, 36 (2019).
35. L. H. Rude, T. K. Nielsen, D. B. Ravnsbæk, U. Bösenberg, M. B. Ley, B. Richter, L. M. Arnbjerg, M. Dornheim, Y. Filinchuk, F. Besenbacher and T. R. Jensen, *Phys. Status Solidi (a)*, **208**, 1754 (2011).
36. R. Peña-Alonso, A. Sicurelli, E. Callone, G. Carturan and R. Raj, *J. Power Sources*, **165**, 315 (2007).
37. Y. S. Wei, W. Meng, Y. Wang, Y. X. Gao, K. Z. Qi and K. Zhang, *Int. J. Hydrogen Energy*, **42**, 6072 (2017).
38. F. Li, Q. Li and H. Kim, *Chem. Eng. J.*, **210**, 316 (2012).
39. G. R. M. Tomboc, A. H. Tamboli and H. Kim, *Energy*, **121**, 238 (2017).
40. Y. V. Larichev, O. V. Netskina, O. V. Komova and V. I. Simagina, *Int. J. Hydrogen Energy*, **35**, 6501 (2010).
41. D. D. Tuan and K. Y. A. Lin, *Chem. Eng. J.*, **351**, 48 (2018).
42. D. D. Tuan, C.-W. Huang, X. Duan, C.-H. Lin and K.-Y. A. Lin, *Int.*

J. Hydrogen Energy, **45**, 31952 (2020).
43. D. D. Tuan and K.-Y. A. Lin, *J. Taiwan Inst. Chem. Eng.*, **91**, 274 (2018).
44. D. D. Tuan, E. Kwon, J.-Y. Lin, X. Duan, Y.-F. Lin and K.-Y. A. Lin, *Chem. Papers*, **75**, 779 (2021).
45. N. Nurlan, A. Akmanova, S. Han and W. Lee, *Chem. Eng. J.*, **414**, 128860 (2021).
46. Y. Chen, W. Yang, S. Gao, Y. Gao, C. Sun and Q. Li, *Sep. Purif. Technol.*, **251**, 117353 (2020).
47. Q. Xiao and S. Yu, *J. Hazard. Mater.*, **418**, 125940 (2021).
48. Y. You, H. Yuan, Y. Wu, Y. Ma, C. Meng and X. Zhao, *Sep. Purif. Technol.*, **264**, 118456 (2021).
49. J. Li, L. He, J. Jiang, Z. Xu, M. Liu, X. Liu, H. Tong, Z. Liu and D. Qian, *Electrochim. Acta*, **353**, 136579 (2020).
50. D. D. Tuan and K.-Y. A. Lin, *Chem. Eng. J.*, **351**, 48 (2018).
51. D. D. Tuan, H. Yang, N. N. Huy, E. Kwon, T. C. Khiem, S. You, J. Lee and K.-Y. A. Lin, *J. Environ. Chem. Eng.*, **9**, 105809 (2021).
52. K.-Y. A. Lin and S.-Y. Chen, *ACS Sustain. Chem. Eng.*, **3**, 3096 (2015).
53. K. Y. A. Lin, J. Y. Lin and H. L. Lien, *Chemosphere*, **172**, 325 (2017).
54. K. Y. A. Lin and C. H. Lin, *Chem. Eng. J.*, **325**, 144 (2017).
55. C. Wu, F. Wu, Y. Bai, B. L. Yi and H. M. Zhang, *Mater. Lett.*, **59**, 1748 (2005).
56. R. Krishna, D. M. Fernandes, C. Dias, J. Ventura, E. Venkata Ramana, C. Freire and E. Titus, *Int. J. Hydrogen Energy*, **40**, 4996 (2015).
57. P. Brack, S. E. Dann and K. G. U. Wijayantha, *Energy Sci. Eng.*, **3**, 174 (2015).
58. J. C. Walter, A. Zurawski, D. Montgomery, M. Thornburg and S. Revankar, *J. Power Sources*, **179**, 335 (2008).
59. T. Wi-Afedzi, E. Kwon, D. D. Tuan, K.-Y. A. Lin and F. Ghanbari, *Sci. Total Environ.*, **703**, 134781 (2020).
60. T. Wi-Afedzi, F.-Y. Yeoh, M.-T. Yang, A. C. K. Yip and K.-Y. A. Lin, *Sep. Purif. Technol.*, **218**, 138 (2019).
61. C.-H. Liu, B.-H. Chen, C.-L. Hsueh, J.-R. Ku, M.-S. Jeng and F. Tsau, *Int. J. Hydrogen Energy*, **34**, 2153 (2009).
62. L. Ai, X. Liu and J. Jiang, *J. Alloys Compd.*, **625**, 164 (2015).
63. B. Cui, G. Wu, S. Qiu, Y. Zou, E. Yan, F. Xu, L. Sun and H. Chu, *Adv. Sustain. Syst.*, **5**, 2100209 (2021).
64. T. Ohno, *Analyst*, **114**, 857 (1989).
65. A.W.W.A.W.E.F. American Public Health Association, Standard Methods for the Examination of Water and Wastewater 22 nd ed., Method 4500-CN- A,B,C,D and E, in, Washington, DC, USA, 4 (2012).

Supporting Information

Catalytic hydrogenation of disinfection by-product bromate by cobalt and nickle prussian blue analogues with borohydride

Po-Hsin Mao*, Young-Kwon Park, Yi-Feng Lin***,†, Bui Xuan Thanh****, Duong Dinh Tuan*****, Afshin Ebrahimi******, Grzegorz Lisak*******,********, Thanit Tangcharoen*********, and Kun-Yi Andrew Lin*,†**

*Department of Environmental Engineering & Innovation and Development Center of Sustainable Agriculture, National Chung Hsing University, 250 Kuo-Kuang Road, Taichung, Taiwan
**School of Environmental Engineering, University of Seoul, Seoul 02504, Korea
***Department of Chemical Engineering and R&D Center for Membrane Technology, Chung Yuan Christian University, 200 Chung Pei Rd., Chungli, Taoyuan, Taiwan
****Faculty of Environment and Natural Resources, Ho Chi Minh City University of Technology, VNU-HCM, 268 Ly Thuong Kiet, District 10, Ho Chi Minh City, 700000, Viet Nam
*****International School, Thai Nguyen University, Thai Nguyen city, 250000, Viet Nam
******Environment Research Center and Department of Environmental Health Engineering Isfahan University of Medical Sciences Isfahan, Iran
*******Residues and Resource Reclamation Centre, Nanyang Environment and Water Research Institute, Nanyang Technological University, Singapore 637141, Singapore
********School of Civil and Environmental Engineering, Nanyang Technological University, Singapore 639798, Singapore
*********Department of Basic Science and Physical Education, Faculty of Science at Sriracha, Kasetsart University, Sriracha Campus, Chonburi, Thailand
(*Received 3 June 2022 • Revised 14 September 2022 • Accepted 31 January 2023*)

S1. Materials

Chemical reagents employed in this study were purchased from commercial suppliers and used directly without further purifications. Cobalt nitrate ($Co(NO_3)_2$) (99.9%) and nickel(II) nitrate ($Ni(NO_3)_2$) (99.9%) were obtained from Sigma-Aldrich (USA). Potassium hexacyanoferrate ($K_3Fe(CN)_6$) (99%) was purchased from J. T. Baker (Germany). Sodium borohydride ($NaBH_4$) (>98%) was received from Acros Orgabics (USA). (Deionized (DI) water was prepared to less than 18 MΩ-cm.

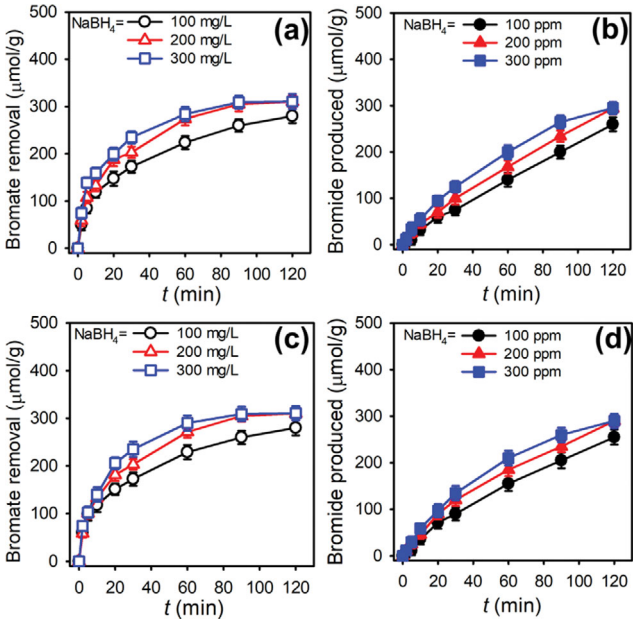

Fig. S1. Effect of $NaBH_4$ concentration on (a) variation of bromate, (b) bromate removal efficiency by CoPB, and (c) variation of bromate, (d) bromate removal efficiency by NiPB (CoPB=NiPB=250 mg/L, T=30 °C).

S2. Preparation and Characterization of PBA

Prussian Blue (PB) analogues were prepared based on the reported protocols [37]. Briefly, 0.02 mol of $K_3[Fe(CN)_6]$ was dissolved to 0.2 L of Deionized (DI) water and the resulting solution was dropwise added to another aqueous solution of 0.2 L of $M^{II}(NO_3)_2$ (0.3 M) (M^{II}=Co, and Ni). The resulting mixture was then aged at ambient temperature for 6 h, and precipitate was then obtained, washed with DI water and dried to afford PBs, including $Co_2[Fe(CN)_6]$, and $Ni[Fe(CN)_6]$, which were denoted as CoPB, and NiPB, respectively.

PBs were then characterized using Powder X-ray diffraction patterns (XRD) of PBs using an X-ray diffractometer (Bruker D8 Discover, USA) to verify their formations. Microscopic images of the as-prepared PBs were visualized using scanning electronic microscopy (SEM). Textural properties of PBs were determined using a volumetric gas adsorption analyzer (Quantachrome Auto IQ, USA) for obtaining N_2 sorption/desorption isotherms. Hydrogen-temperature-programmed reduction (H2-TPR) properties of PBs were also analyzed by using a volumetric gas adsorption analyzer equipped with a TCD detector (Quantachrome TPX, USA)

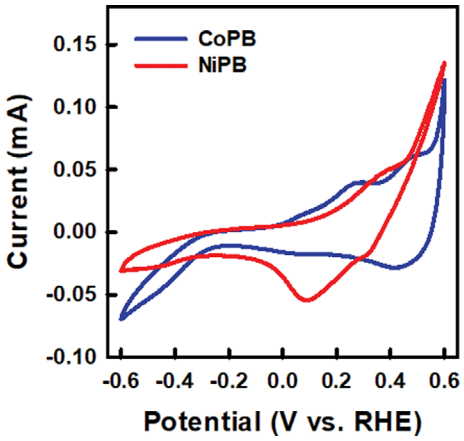

Fig. S2. CV curves of CoPB, and NiPB.

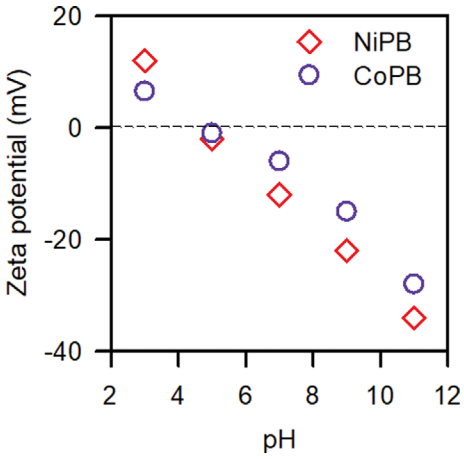

Fig. S3. Zeta potentials of CoPB, and NiPB in water.

to reveal redox properties of PBs. Surface chemistry of PBs was analyzed using X-ray photoelectron spectroscopy (XPS) (ULVAC-PHI, Inc., Japan). N_2 sorption isotherm and pore size distribution were determined using a volumetric gas adsorption analyzer (Anton Paar ASIQ, USA). Surface charges of PBs were measured using a zetasizer (Malvern Nano S, UK).

S3. Catalytic Hydrogenation of Bromate Using PB

Bromate removal efficiency, and bromide production efficiency were determined by the following equation:

$$q_t = \frac{v|C_0 - C_t|}{M}$$

where M (g) is the amount of PB used in the reduction experiment and v (L) is the total volume of solution. C_t denotes the concentration of bromate (or bromide) at a given reaction time t, was expressed in mmol/L and so was C_0 (mmol/L), the initial concentration of bromate (or bromide). The q_e was used to express bromate removal efficiency, or bromide production efficiency at equilibrium. An initial bromate concentration of 10 mg/L (i.e., 0.078 mM) was employed as this concentration has been extensively used as a model in published studies [23,35,36].

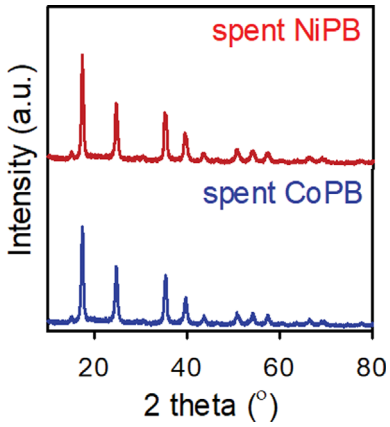

Fig. S4. XRD patterns of spent CoPB, and NiPB.

S4. Analytic Methods

The concentrations of Co and Ni found in the solution were determined using Inductively coupled plasma mass spectrometry (ICP-MS) (ICP-MS ELEMENT^{TM} GD PLUS GD, ThermoFisher, USA). For determining the concentration of cyanide ion in water, a spectrophotometric method was adopted by using a pyridine-barbituric acid reagent. When cyanide reacts with chloramine-T, the addition of the pyridine-barbituric acid reagent would result in a soluble violet-blue product, which is measured at 578 nm for quantifying the presence, and concentration of cyanide ion [5,6].

S5. DFT Calculation for Adsorption of Borohydrides onto PB

The DFT calculation was performed using the DMol^3 software package and a basis set of dual numerical polarization DNP was employed for calculation of all atoms with unrestricted electron spin. The generalized gradient correction and Perdew-Burke-Ernzerhof function were adopted to approximate exchange and correlation [34,35]. PB (200) was selected as a representative plane to create the supercell with a vacuum thickness of 10 Å. The adsorption energy of borohydride to PB (200) was quantified by the following equation:

$$\text{Adsorption energy} = E_{borohydride@PB(200)} - E_{borohydride} - E_{PB(200)}$$